Available online at www.sciencedirect.com
SCIENCE DIRECT
Journal of Power Sources 150 (2005) 20–26
JOURNAL OF POWER SOURCES
www.elsevier.com/locate/jpowsour

# Preparation of $Cu/ZnO/Al_2O_3$ catalyst for a micro methanol reformer

Yoshihiro Kawamura [a,*], Kazuto Yamamoto [a], Naotsugu Ogura [a], Takashi Katsumata [b], Akira Igarashi [b]

[a] *CASIO Computer Co. Ltd., 10-6 Imai 3-chome, Ome-shi, Tokyo 198-8555, Japan*
[b] *Department of Environmental Chemical Engineering, Kogakuin University, 2665-1 Nakano-machi, Hachioji-shi, Tokyo 192-0015, Japan*

Received 12 July 2004; received in revised form 22 September 2004; accepted 21 February 2005
Available online 2 April 2005

**Abstract**

A $Cu/ZnO/Al_2O_3$ catalyst suitable for low-temperature methanol reforming is proposed. The catalyst achieved by optimization of the temperature and pH of preparation and the addition of boehmite has superior catalytic activity to commercial catalysts. The catalytic activity is found to depend on the Cu surface area, which is related to the amount of Cu dispersed within ZnO. Dispersion of Cu is promoted by precipitation at low temperature, which results in the formation of small crystallites of the precursor. Enlarged BET surface area by the addition of boehmite as the third component derives high catalytic activity. Under optimized pH, it is predicted that the excess of Cu species existing as amorphous-like malachite in the precursor, in addition to aurichalcite, facilitates the dispersion of Cu. The proposed catalyst system can achieve methanol reforming at temperatures 20–25 °C lower than conventional catalysts, representing an improved source of $H_2$ for small proton exchange membrane fuel cell systems.


*Keywords:* Cu/ZnO catalyst; Hydrogen production; Methanol reforming; Cu dispersion; Microreformer; Fuel cell

## 1. Introduction

The high power consumption of modern portable electronic devices such as laptop computers and digital cameras has given rise to a need for high-efficiency power sources. Furthermore, the manufacture of the conventional dry batteries used for portable electronic devices consumes large amounts of energy, and environmental pollution from the mass disposal of these cells is a concern. Small proton exchange membrane fuel cell (PEMFC) systems have therefore been developed as a substitute for conventional dry batteries as a power source for portable electronic devices.

The two types of small PEMFC systems currently under development are the direct methanol type and the reforming type. In the direct methanol system, fuel-containing methanol is directly decomposed over a catalyst deposited on the polymer electrolyte membrane. Although direct methanol systems have the advantage of room-temperature operation, they offer only relatively low power density due to methanol crossover through the polymer electrolyte membrane and the low reaction rate of methanol oxidation over an anode electrocatalyst. In contrast, in reforming systems, the electronic energy is generated using concentrated hydrogen produced by steam reforming from a fuel such as methanol. Reforming systems can achieve high power densities, but are difficult to be miniaturized due to the complicated structure of the reformer. In addition, methanol reforming, for example, requires temperatures of up to 300 °C.

Recently, however, attempts have been made to miniaturize the complicated reformer for application as a small power source [1,2], and it appears likely that a microreactor [3], which has several advantages over a conventional reactor, may be realized using microfabrication technology. To apply the miniaturized reformer as a power source for portable electronic devices and maintain high energy efficiency, hydrogen production at lower temperature is required because of the

* Corresponding author. Tel.: +81 428 32 1741; fax: +81 428 31 7651.
*E-mail address:* kawamuy@rd.casio.co.jp (Y. Kawamura).

0378-7753/$ – see front matter © 2005 Elsevier B.V. All rights reserved.
doi:10.1016/j.jpowsour.2005.02.030

increased heat release of miniaturized reactors, which have high specific surface area.

Methanol is expected to be an appropriate fuel for the microreformer because of the feasibility of hydrogen production at low temperature [1]. Methanol steam reforming is an endothermic reaction, as given by

$$CH_3OH + H_2O \rightarrow 3H_2 + CO_2,$$
$$\Delta H^0_{298} = 49.5\,\mathrm{kJ\,mol^{-1}} \quad (1)$$

Cu/ZnO catalysts and precious-metal catalysts such as Pd are typically used for methanol reforming. Cu/ZnO catalysts are employed in current commercial processes, and can achieve reforming at relatively low temperatures of below 300 °C. Moreover, as the equilibrium concentration of CO depends on the reforming temperature, a Cu/ZnO catalyst used at low temperature has the advantage of low CO concentration (approximately 1 mol% of the produced gas), preventing deterioration of the anode. The need for only a preferential oxidation of CO (PROX) process for gas purification prior to supply to a fuel cell makes this system suitable for the realization of small reformer requiring a simple system. Although precious-metal catalysts have superior thermal stability, they do not provide sufficient catalytic activity or CO selectivity compared to the Cu/ZnO catalyst system [4], requiring temperatures for methanol steam reforming. Cu/ZnO catalysts have been studied for use in methanol synthesis, water gas shift reaction, and methanol steam reforming [4–12]. However, there are few reports on the development of the catalyst for low-temperature hydrogen production as required for miniaturized methanol reformers, and the applicability as a power source for portable electronic devices is yet to be discussed.

In this paper, as part of development of a small methanol reformer for the supply of hydrogen to a small PEMFC, the preparation of a Cu/ZnO catalyst with superior catalytic performance for methanol reforming at low temperature is presented.

## 2. Experimental

### 2.1. Catalyst preparation

The Cu/ZnO/$Al_2O_3$ catalysts were prepared by coprecipitation. $Al_2O_3$ was prepared by precipitation as a third component. An aqueous solution of $Na_2CO_3$ (0.76 M) was added dropwise to an aqueous solution of aluminum nitrate (1.4 M) at 60 °C under continuous stirring, and the resulting precipitate was filtered out three times, washing for 20 min between each filtering step. The precipitate was then dried for 12 h at 100 °C and calcined under air flow for 1 h at 360 °C.

A mixed solution of copper and zinc nitrate (total 1.8 M) at 60 °C and an aqueous solution of $Na_2CO_3$ (0.76 M) were then simultaneously added to a suspension of prepared $Al_2O_3$ in a dropwise manner under continuous stirring and at a prescribed temperature. The volumes of the solutions were adjusted such that the atomic ratio of Cu/Zn/Al was 6/3/1 (mole ratio). During precipitation, the pH of the suspension was monitored using a pH meter, and $Na_2CO_3$ solution was added at a controlled rate so as to maintain the prescribed pH. After stirring for 60 min, the precipitate was aged for 12 h at room temperature, and then filtered out five times, washing for 20 min between each filtering step. The washing temperature was 90 °C for the first wash and then 60 °C for all subsequent washes. The cake collected from the precipitate was dried for 12 h at 100 °C and calcined under air flow for 1 h at 360 °C to afford the Cu/ZnO/$Al_2O_3$ catalyst, which was then pelletized under a pressure of $3.5 \times 10^8$ Pa to give a uniform 0.5–1.0 mm powder.

The effect of precipitation temperature was examined by precipitating the catalysts at 60 °C (catalyst A) and 90 °C (catalyst B) at a pH of 9.4. The effect of adding $Al_2O_3$ was examined by preparing catalysts with $Al_2O_3$ as above (catalyst C), γ-$Al_2O_3$ (JRC-ALO-6, reference catalyst of the Catalysis Society of Japan) at pH 9.3 and 60 °C (catalyst D, respectively), and without an additive (catalyst E). To examine the effect of pH, four catalysts with $Al_2O_3$ prepared by precipitation were prepared at pH from 8.0 to 9.2 at 60 °C (catalysts F–I).

### 2.2. Catalytic performance test

Performance tests were carried out using a conventional fixed-bed flow reactor (SUS304, 8 mm internal diameter). The catalyst was placed in the reactor and reduced under 60 ml $min^{-1}$ $H_2$ flow at 300 °C for 1 h. The catalyst bed was then cooled to 200 °C under $N_2$ flow for 20 min, after which a mixed solution of methanol and water (steam/methanol = 2 (mole ratio)) was fed into the reactor at a gas space velocity of 100,000 $h^{-1}$ through a vaporizer heated to 110 °C. The catalytic performance was measured at every 25 °C step up to 300 °C. The gases produced were analyzed using a gas chromatograph (column, active carbon; 3.0 mm internal diameter × 3.5 m length; carrier gas, He) with thermal conductivity detector.

### 2.3. Characterization of catalyst

BET surface areas of the calcined catalysts and $Al_2O_3$ as an additive component were determined by $N_2$ adsorption at −196 °C using a flow absorption apparatus (Flow Sorb II, Micromeritics). Measurement of the samples was carried out under a flow of mixed gas ($N_2$:He = 3:7). Prior to measurement, samples were degassed at 200 °C for 20 min under mixed gas flow as above.

X-ray diffraction (XRD) analysis of the catalysts and precursors was carried out using an X-ray diffractometer (RINT2000, Rigaku). The sizes of ZnO(1 0 0) crystallite in the calcined catalysts and malachite ($Cu_2CO_3(OH)_2$) (1 2 0)

and CuO(1 1 1) crystallites in the precursor were calculated using the Scherrer equation.

The Cu surface area of the catalyst was measured based on Cu oxidation by $N_2O$ titration using a fixed-bed flow reactor [13–15]. $N_2O$ as an oxidant and $N_2$ produced by Cu oxidation were detected using a quadrupole mass spectrometer [16] (AQA-100MPX, Anelva). For the estimation of the Cu surface area by $N_2O$, a mass spectrometer, which performs the simultaneous detection of several components, is a suitable apparatus to observe both of $N_2O$ and $N_2$ produced by the oxidation of Cu. However, in order to establish accuracy of the measurement using a mass spectrometer, it is necessary to consider fragmentation from $N_2O$ at a quadrupole analyzer. Then, as a pre-experiment, the ratio of ions fragmented from $N_2O$ was evaluated using an inert reactor tube filled with quartz sand instead of catalyst. The result showed that the ratio of observed spectra derived from N ($m/e = 14$), O ($m/e = 16$), $N_2$ ($m/e = 28$), and NO ($m/e = 30$), in addition to $N_2O$ ($m/e = 44$) was constant stably. And further, it was confirmed that the intensity of the observed $N_2O$ spectrum was proportional to the amount of introduced $N_2O$. Therefore, the amount of consumed $N_2O$ for the Cu oxidation could be analyzed quantitatively as a differential of the detected spectrum area of $N_2O$ from the criterial spectrum area, which was determined as a spectrum area at the saturation of the titration. And, the $N_2$ spectrum should inform the stability of fragmentation during the measurement for the further confirmation of the accurate quantifiability. Hence, the unsoundness caused by fragmentation in the mass spectrometer was thought to be excluded. Next, the estimation of Cu surface area of the prepared catalyst was employed actually. After placing the catalyst into a reactor tube, the catalyst was reduced under 60 ml $min^{-1}$ $H_2$ flow for 15 min at 300 °C at a programmed heating rate of 10 °C $min^{-1}$. The reactor was then cooled to 60 °C and maintained at that temperature. A 0.1 ml dose of $N_2O$ was then injected by microsyringe into the 60 ml $min^{-1}$ He stream, which was purified through an $O_2$ trap consisted of a manganese oxide bed. This dosing was repeated at intervals of 5 min until the $N_2O$ spectrum reached saturation. The Cu surface area was estimated stoichiometrically (Cu/O = 2) based on the amount of $N_2O$ consumed to oxidize the Cu surface discussed above of the catalyst [17]. The turnover frequency (TOF) was calculated based on methanol conversion and the Cu surface area.

A transmission electron microscope (TEM; HF-2000, Hitachi) and an energy dispersive X-ray (EDX) fluorescence spectrometer (M3100, Noran) were used to observe the microscopic structure and to determine the chemical composition of the calcined catalyst.

A temperature programmed reduction (TPR) spectrum of the catalyst was measured by thermogravimetry differential thermal analysis (TG/DTA; TG–DTA2010, Mac Science). TG analysis of the calcined catalyst was carried out under 60 ml $min^{-1}$ $H_2$ flow at a programmed heating rate of 5 °C $min^{-1}$.

Table 1
Precipitation conditions and catalytic activity of $Cu/ZnO/Al_2O_3$ catalyst

| Catalyst | Precipitation condition | | $Al_2O_3$[a] | Methanol conversion at 250°C (%) |
|---|---|---|---|---|
| | Temperature (°C) | pH | | |
| A | 60 | 9.4 | (1) | 68.6 |
| B | 90 | 9.4 | (1) | 55.7 |
| C | 60 | 9.3 | (1) | 78.4 |
| D | 60 | 9.3 | (2) | 67.7 |
| E | 60 | 9.3 | No additive | 56.9 |
| F | 60 | 9.2 | (1) | 82.5 |
| G | 60 | 8.8 | (1) | 84.3 |
| H | 60 | 8.4 | (1) | 78.6 |
| I | 60 | 8.0 | (1) | 71.4 |

[a] (1) Boehmite and (2) JRC-ALO-6.

## 3. Results and discussion

### 3.1. Relationship between preparation conditions and catalytic performance

The preparation conditions and catalytic activities of the prepared catalysts are listed in Table 1. As can be seen from the table, catalyst A, prepared at 60 °C, exhibited higher catalytic activity than catalyst B (90 °C). Catalyst C, containing prepared $Al_2O_3$ (identified as boehmite by XRD), exhibited superior catalytic activity to catalyst D ($\gamma$-$Al_2O_3$) and catalyst E (no additive), and catalyst G, prepared under conditions of pH 8.8, had superior catalytic activity to any of the catalysts prepared at other pH levels.

Fig. 1 shows a comparison of the catalytic performance of a commercial catalyst (MDC-3, Süd-Chemie) with that of catalyst G, which had the highest catalytic activity of any of the catalysts prepared in this study. The figure clearly shows that the $Cu/ZnO/Al_2O_3$ catalyst prepared under optimal conditions has superior catalytic activity compared to the commercial catalyst. At a given temperature, the CO selectivity of the prepared catalyst was also greater than that of the commercial catalyst. A Cu/ZnO catalyst having high catalytic activity for methanol reforming also performs effectively for water gas shift reaction, in other words, reverse water gas

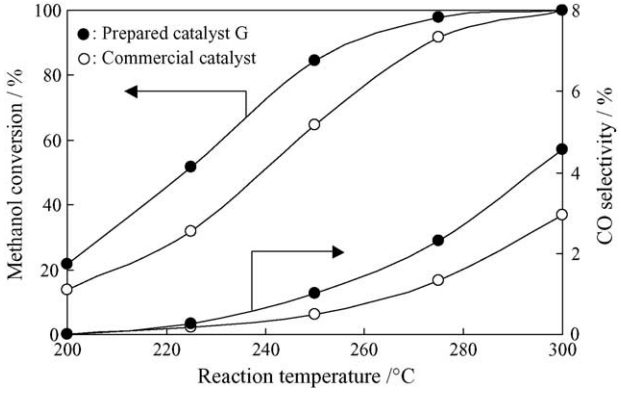


Fig. 1. Catalytic performances of prepared catalyst G and commercial catalyst.

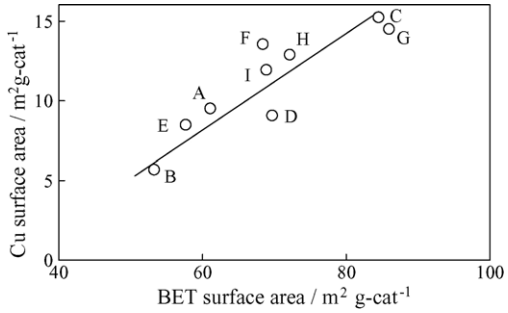


Fig. 2. Relationship between BET surface area and Cu surface area.

shift reaction should be advanced. Therefore, increase of CO concentration over the optimized catalyst is inevitable. Nevertheless, the CO selectivity of 3%, corresponding to the CO concentration of approximately 0.8%, over the catalyst G at 280 °C, at which the methanol conversion reached to almost 100%, was sufficiently low to decrease with only a PROX process in a miniaturized methanol reforming system. These results show that the catalyst prepared in this study achieves methanol conversion equivalent to the commercial catalyst at about 20–25 °C lower. In the case of methanol steam reforming in a miniaturized reformer, which has larger specific surface area than a conventional reactor, operation at low temperature is particularly effective with regard to energy efficiency.

### *3.2. Influence of catalyst characteristics on catalytic activity*

The relationship between catalyst properties and catalytic activity was examined based on the BET surface area and Cu surface area of the prepared catalysts. As shown in Fig. 2, the Cu surface area was found to increase with the BET surface area. Furthermore, as shown in Fig. 3, the catalytic activity increased with the Cu surface area, whereas the TOF remained constant. Therefore, the catalytic activity appears to depend on the amount of active sites related to the Cu surface area, which was enhanced by increasing the BET surface area.

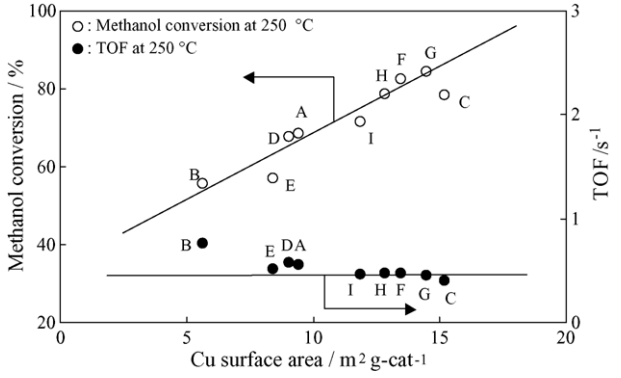


Fig. 3. Influence of Cu surface area on catalytic activity and TOF.

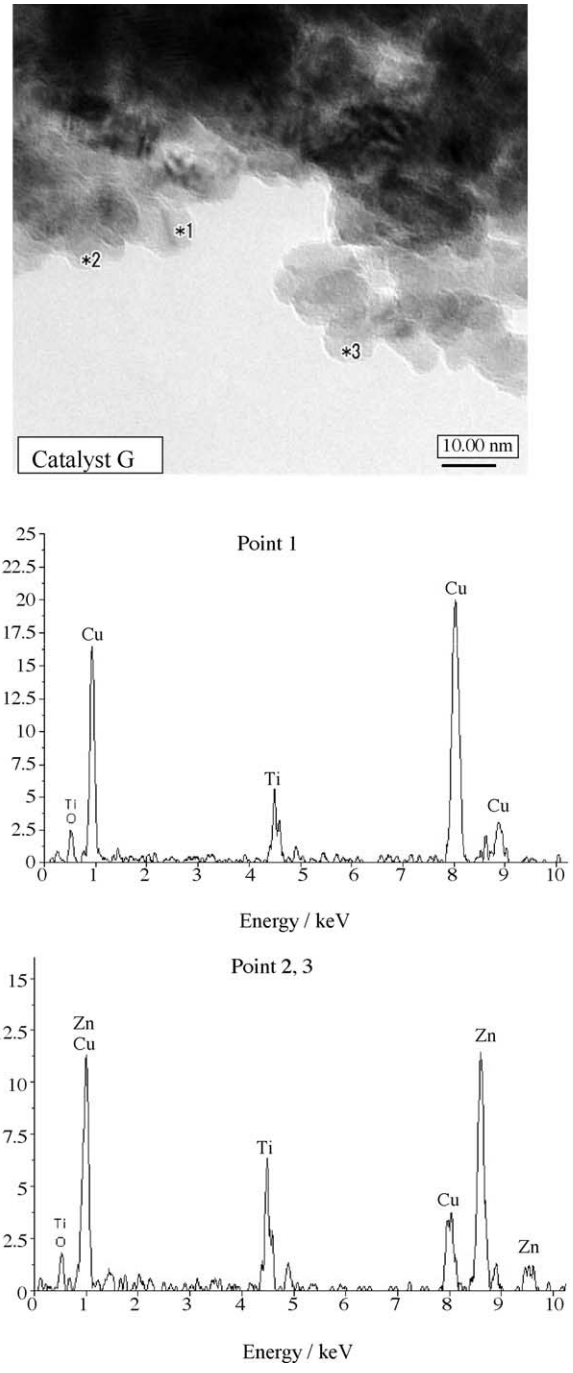


Fig. 4. Composition of particles of catalyst G analyzed by TEM–EDX.

Fig. 4 shows the results of analyses of the microscopic structure and chemical composition of catalyst G by TEM and EDX. The dimensions of the particles observed by TEM almost correspond to the crystallite sizes of ZnO and CuO estimated by XRD. EDX analyses of the three points in the figure identified the sites to consist of Cu (point 1) or Cu and Zn (points 2 and 3). The peaks identified as Ti were caused by scattering from the titanium specimen holder. The active sites of the $Cu/ZnO/Al_2O_3$ catalyst therefore appear to be fine Cu species highly interdispersed with ZnO, as indicated

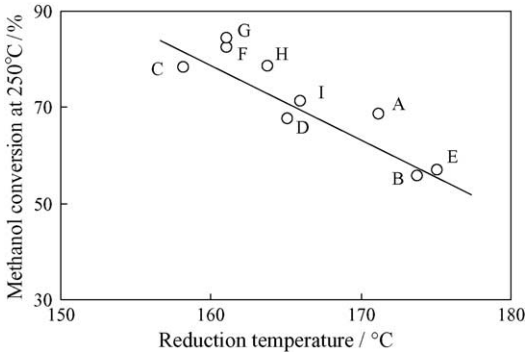


Fig. 5. Relationship between reduction temperature measured by TPR and catalytic activity.

by points 2 and 3, in addition to crystallized Cu as indicated by point 1. This expectation agrees with the report [7], which describes the importance of the fine interdispersion between Cu and ZnO.

The relationship between the catalytic activity of the catalyst and the reduction temperature measured by TPR is shown in Fig. 5. Also, TPR profiles observed as DTA curves with temperatures are shown in Fig. 6. The reduction temperature was determined as the peak observed at the lowest temperature among the exothermic peaks of $H_2$ oxidation during reduction of catalyst. Catalysts with higher catalytic activity were found to have lower reduction temperature, attributable to smaller sizes of Cu particles due to thermodynamic instability. Therefore, it is predicted that the fine Cu particles predominantly govern the catalytic activity, and a part of such small Cu particles probably present as fine Cu species interdispersed in the ZnO since the result of the TEM–EDX analyses discussed above. The weight loss of the catalyst by reduction, as measured by TG analysis, was approximately 12.8 wt%, corresponding to the stoichiometric ratio under the assumption of reduction from CuO to Cu. Therefore, the Cu component in the calcined catalyst, including the fine Cu species, exists as CuO.

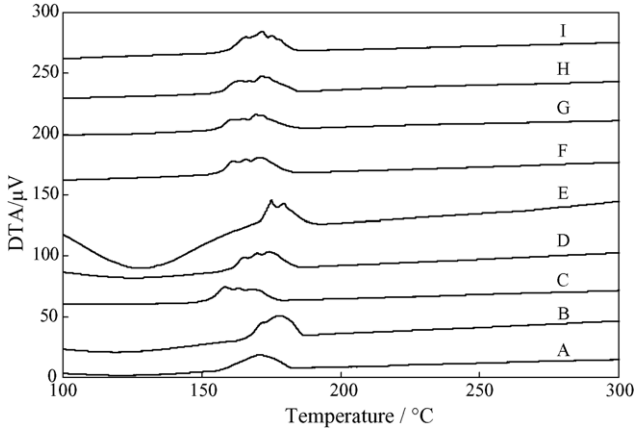


Fig. 6. TPR profiles of prepared catalysts measured by TG–DTA.

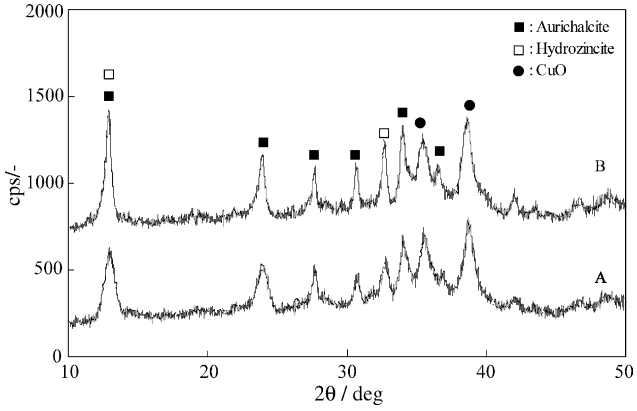


Fig. 7. Effect of precipitation temperature on precursor formation.

### 3.3. Influence of preparation conditions on dispersion of Cu

XRD analysis of the precipitates as precursors was carried out in order to investigate the influence of the preparation conditions on the dispersion of Cu in the final catalyst. The XRD profiles of the precursors of catalysts A and B, which were prepared at different precipitation temperatures, are shown in Fig. 7. Both precursors consist of aurichalcite ($(Cu, Zn)_5(CO_3)_2(OH)_6$), hydrozincite ($Zn_5(CO_3)_2(OH)_6$), and CuO. However, the peaks in the spectrum for the precursor of catalyst A (60 °C) are broader than those for catalyst B (90 °C). As catalyst A exhibited higher catalytic activity than catalyst B, the high dispersion of Cu in the former is probably due to the small crystallite size in the precipitate by slow formation at low temperature. Among the three crystal phases detected in the precursors, the phase related to the interdispersion of Cu and ZnO is thought to be aurichalcite, based on its chemical composition. It has been reported that Cu/ZnO catalysts prepared from aurichalcite exhibit high catalytic activity [4,7]. The present results suggest that the formation of small aurichalcite crystallite through optimization of the precipitation conditions is effective for preparing Cu/ZnO/$Al_2O_3$ catalysts with even higher catalytic activity.

Fig. 8 shows a comparison of the XRD profiles for the precursors of catalyst C (prepared with boehmite), catalyst

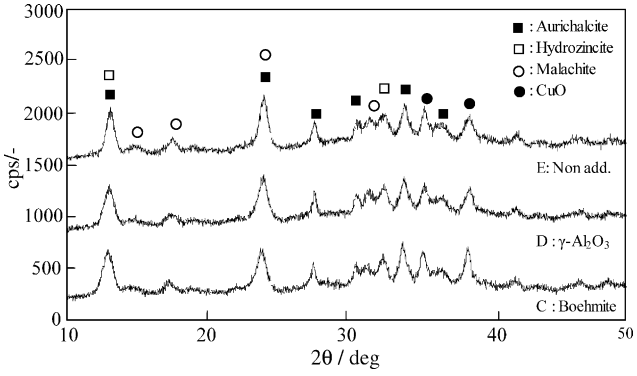


Fig. 8. Effect of addition of $Al_2O_3$ on precursor formation.

Table 2
Effect of BET surface area and addition of $Al_2O_3$ on catalytic activity

| Catalyst | $Al_2O_3$ | Methanol conversion[a] (%) | BET surface area of $Al_2O_3$ ($m^2\ g^{-1}$) |
|---|---|---|---|
| C | Prepared boehmite | 78.4 | 172.8 |
| D | $\gamma$-$Al_2O_3$[b] | 67.7 | 158.0 |
| E | None | 56.9 | – |

[a] At 250 °C.
[b] JRC-ALO-6.

D (prepared with $\gamma$-$Al_2O_3$), and catalyst E (no additive). Although these three catalysts were prepared from very similar precursors, catalyst C exhibited the highest catalytic activity among these three catalysts. Boehmite has a larger BET surface area than $\gamma$-$Al_2O_3$, as shown in Table 2, indicating that while the addition of $Al_2O_3$ and the kind of $Al_2O_3$ have no effect on the precursor selectivity; the addition of $Al_2O_3$ increases the surface area of the catalyst, bringing about higher catalytic activity.

Fig. 9 shows the relationship between the Cu surface area and the size of ZnO crystallites estimated from the XRD profiles of the calcined catalysts A–C and E–I, which included boehmite. As described above, the abundance of active sites related to the Cu surface area affects the catalytic activity, and the Cu surface area itself is correlated with the size of ZnO crystallites in the comparison between catalysts A and B. This is probably due to formation of small aurichalcite crystallites (resulting in small ZnO crystallites) as a result of the slow rate of precursor formation at low precipitation temperature. Therefore, appropriate selection of the precipitation temperature leads to higher surface area and smaller ZnO crystallites, resulting in higher Cu surface area in the catalyst through the dispersion of fine Cu species.

In contrast, the size of ZnO crystallites in catalysts A, C, and F–I, which were prepared at different precipitation pH, appears to be independent of the Cu surface area in Fig. 9. Fig. 10 shows a comparison of the XRD profiles for the precursor of catalysts A, C, and F–I. While aurichalcite and hydrozincite were observed over a wide range of pH (8.0–9.4), malachite as a cupric component was detected

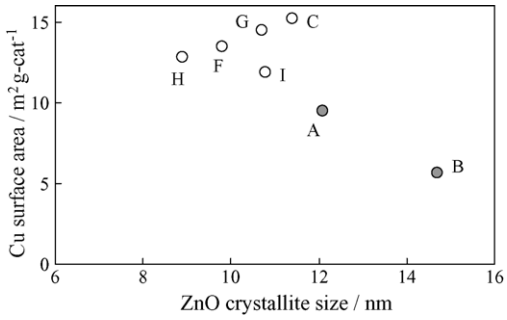


Fig. 9. Relationship between size of ZnO crystallite and Cu surface area.

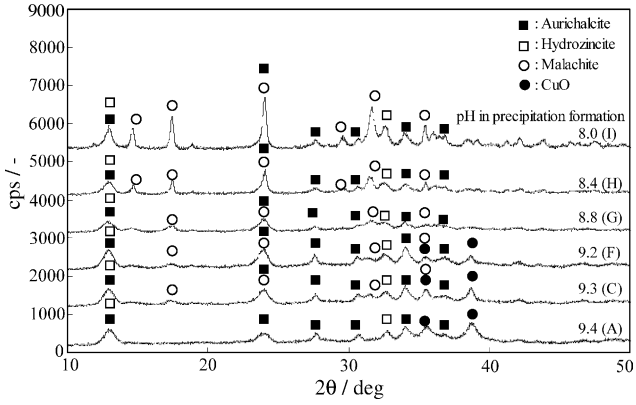


Fig. 10. Effect of precipitation pH on precursor formation.

only in the precursors prepared at pH 9.3 or below, and CuO as a source of cupric compounds was only observed in catalysts prepared at pH 9.2 or above. The size of CuO and malachite crystallites was estimated from the XRD profiles. According to the results shown in Fig. 11, the minimum crystallite sizes for CuO and malachite, and hence maximum catalytic activity, are obtained at pH 8.8. It has been reported that $Cu^{2+}$ in precipitates transforms into malachite through anion exchange with copper hydroxy carbonate ($Cu_2(OH)_{4-2x}(CO_3)_x$), which replaces part of $OH^-$ in amorphous $Cu(OH)_2$ with $CO_3^{2+}$ [5]. When precipitation is carried out at high pH, the high concentration of $OH^-$ in solution suppresses the replacement of $OH^-$ in $Cu(OH)_2$, preventing the transformation to malachite. Hence, it is thought that crystallization of CuO proceeds by the decomposition of intermediates at high pH. In contrast, in the case of catalysts prepared at the low precipitation pH, crystallization of malachite tends to progress. As an intermediary phase between copper hydroxy carbonate and malachite, the presence of georgeite, which has identical composition with malachite but amorphous phase, has been suggested [7]. Also, it has been evidenced that zinc can be partially substituted of cop-

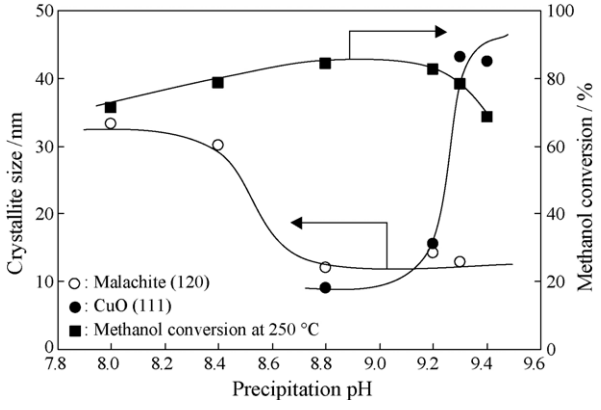


Fig. 11. Effect of precipitation pH on catalytic activity and sizes of malachite and CuO crystallite in precursor.

per in georgeite to form zincian-georgeite, which transforms into malachite slowly [18]. Therefore, the precipitation of amorphous-like phase of malachite in the precursor precipitated at pH 8.8 still contains a small amount of Zn probably, and hence is thought to be responsible for further interdispersion of Cu and ZnO resulting high catalytic activity.

## 4. Conclusions

A Cu/ZnO/$Al_2O_3$ catalyst capable of methanol reforming at temperatures 20–25 °C lower than commercial catalysts was successfully developed. This catalyst provides enhanced energy efficiency for applications, such as miniaturized reformers, which have large specific surface area. Copper as active sites was found to be interdispersed with small ZnO crystallites, and the catalytic activity was found to depend on the Cu surface area, which is in turn related to the amount of dispersed Cu. A catalyst prepared from a precursor containing small aurichalcite crystallite provided high catalytic activity. In addition, the dispersion of Cu species present as amorphous-like malachite in the precursor is effective for preparing catalysts with high catalytic activity. The optimal conditions of precipitation temperature and pH were identified for the preparation of this precursor. The addition of boehmite, which has high surface area, provides higher catalytic activity through an increase in the BET surface area of the final catalyst.

## References

[1] J.D. Holladay, E.O. Jones, M. Phelps, J. Hu, J. Power Sources 108 (2002) 21–27.
[2] J. Hu, Y. Wang, D. VanderWiel, C. Chin, D. Palo, R. Rozmiarek, R. Dagle, J. Cao, J. Holladay, E. Baker, Chem. Eng. J. 93 (2003) 55–60.
[3] W. Ehrfeld, V. Hessel, H. Löwe, Microreactors, Wiley–VCH, Weinheim, Germany, 2000.
[4] N. Iwasa, W. Nomura, T. Mayanagi, S. Fujita, M. Arai, N. Takezawa, J. Chem. Eng. Jpn. 37 (2004) 286–293.
[5] G.C. Shen, S. Fujita, N. Takezawa, J. Catal. 138 (1992) 754–758.
[6] S. Fujita, A.M. Satriyo, G.C. Shen, N. Takezawa, Catal. Lett. 34 (1995) 85–92.
[7] T. Matsuhisa, in: J.J. Spivey (Ed.), Catalysis, vol. 12, The Royal Society of Chemistry, Cambridge, 1996, pp. 1–20.
[8] K. Klier, in: D.D. Eley, H. Pines, P.B. Weisz (Eds.), Advances in Catalysis, vol. 31, Academic Press, New York, 1982, pp. 243–313.
[9] G. Ghiotti, F. Boccuzzi, Catal. Rev. Sci. Eng. 29 (1987) 151–182.
[10] J. Agrell, H. Birgersson, M. Boutonett, I. Melián-Cabrera, R.M. Navarro, J.L.G. Fierro, J. Catal. 219 (2003) 389–403.
[11] P.H. Matter, D.J. Braden, U.S. Ozkan, J. Catal. 223 (2004) 340–351.
[12] T. Shishido, Y. Yamamoto, H. Morioka, K. Takaki, K. Takehira, Appl. Catal. A: Gen. 263 (2004) 249–253.
[13] J.J.F. Scholten, J.A. Konvalinka, Trans. Faraday Soc. 65 (1969) 2465–2473.
[14] J.W. Evans, M.S. Wainwright, A.J. Bridgewater, D.J. Young, Appl. Catal. 7 (1983) 75–83.
[15] G.C. Chinchen, C.M. Hay, H.D. Vandervell, K.C. Waugh, J. Catal. 103 (1987) 79–86.
[16] K.J. Soerensen, N.W. Cant, Catal. Lett. 33 (1995) 117–125.
[17] S. Fujita, S. Matsumoto, N. Takezawa, Catal. Lett. 25 (1994) 29–36.
[18] A.M. Pollard, M.S. Spencer, R.G. Thomas, P.A. Williams, J. Holt, J.R. Jennings, Appl. Catal. A: Gen. 85 (1992) 1–11.